Comprehensive Histopathological and Immunohistochemical Evaluation of African Swine Fever in Romanian Swine: Insights into Pathogenesis and Diagnostic Strategies

Andrei Ungur *, Andras-Laszlo Nagy, Cornel Cătoi *

Posted Date: 23 November 2023

doi: 10.20944/preprints202311.1487.v1

Keywords: African Swine Fever; Histopathology; Immunohistochemistry; Tissue-specific prevalence

Article

Comprehensive Histopathological and Immunohistochemical Evaluation of African Swine Fever in Romanian Swine: Insights into Pathogenesis and Diagnostic Strategies

Andrei Ungur [1,*], Andras Nagy [2,3] and Cornel Cătoi [4,*]

[1] Department of Porcine Health Management, Faculty of Veterinary Medicine, University of Agricultural Sciences and Veterinary Medicine of Cluj-Napoca, 400372 Cluj-Napoca, Romania; andrei.ungur@usamvcluj.ro

[2] Department of Biomedical Sciences, Ross University School of Veterinary Medicine, Basseterre P.O. Box 334, Saint Kitts and Nevis, email: anagy@rossvet.edu.kn

[3] Department of Toxicology, Faculty of Veterinary Medicine, University of Agricultural Sciences and Veterinary Medicine of Cluj-Napoca, 400372 Cluj-Napoca, Romania;

[4] Department of Porcine Health Management, Faculty of Veterinary Medicine, University of Agricultural Sciences and Veterinary Medicine of Cluj-Napoca, 400372 Cluj-Napoca, Romania; cornel.catoi@usamvcluj.ro

* Correspondence: A.U. e-mail: andrei.ungur@usamvcluj.ro, +40745913324; C.C. e-mail:cornel.catoi@usamvcluj.ro

Simple Summary: This research investigated African Swine Fever (ASF) in domestic pigs, focusing on histopathological changes and employing immunohistochemistry for virus detection. Tissue samples from ASF-positive pigs were examined, revealing significant findings. The study identified key affected organs such as lymph nodes, spleen, and kidneys, showing prominent vascular involvement and consequential lesions. Hemorrhagic manifestations were notable in the spleen (93.1%), kidneys (87.7%), and lymph nodes (83.7%). Necrotic lesions were prevalent in the spleen (68.1%), lymph nodes (61.5%), and tonsils (53.9%). Microthromboses were also observed, particularly in lymph nodes (57.2%) and kidneys (50.8%). Immunohistochemistry successfully detected the ASF virus across all examined organs, emphasizing its presence in specific cell types. Tonsils consistently exhibited the highest viral presence. The study contributes valuable insights into ASF pathogenesis, highlighting organ-specific patterns and emphasizing the diagnostic robustness of immunohistochemistry, even in the presence of tissue autolysis. These findings enhance our understanding of ASFV distribution and its impact on affected organs.

Abstract: African Swine Fever (ASF) poses a significant threat to domestic pig populations worldwide. This study investigates the histopathological alterations in confirmed ASF-positive domestic pigs, focusing on over 100 cases from 2018 to 2021. Biological material from 118 pigs, confirmed ASF-positive via PCR examination, was histopathologically examined. Tissue samples from various organs were processed, embedded, and analyzed using hematoxylin and eosin staining. Immunohistochemistry (IHC) was employed to detect the major capsid protein (p72) of the ASF virus.Histological examination revealed characteristic ASF lesions, including severe hemorrhages, lymphoid depletion, and inflammatory infiltrates. Vascular anomalies leading to hemorrhagic events were widespread. Microthromboses were prevalent in lymph nodes and kidneys. IHC detected p72 in various organs, with tonsils consistently showing the highest viral presence.This comprehensive study underscores the pivotal role of lymph nodes, spleen, and kidneys in ASF pathogenesis, highlighting prominent vascular involvement and hemorrhagic manifestations. The study establishes the efficacy of IHC in detecting ASF virus, even in autolyzed tissue samples. Tonsils emerge as a consistent epicenter of viral presence, shedding light on the intricate pathogenesis of ASFV.

Keywords: African Swine Fever; Histopathology; immunohistochemistry; tissue-specific prevalence

 doi:10.20944/preprints202311.1487.v1

1. Introduction

African Swine Fever (ASF) is a viral hemorrhagic malady affecting swine, and its pervasive spread across Europe has led to considerable disruptions in pig production, economic sectors, and the trade of pig and pork products, consequently influencing social well-being within affected regions [1]. The causative agent of this disease, the ASF virus, is a large, intricate, enveloped DNA virus classified within the Asfarviridae family and Asfivirus genus. It is distinguished for its remarkable environmental stability [2; 3]. The infectious ASF virus can persist in pig tissues for extended periods, particularly in tissues like blood, muscle, or skin stored at temperatures of -20 or 4 °C [4]. The malady affects both wild and domestic pig populations, commonly exhibiting an acute course, with infected animals displaying hyperthermia, anorexia, cutaneous hyperemia, and respiratory and vascular disorders. The mortality rate can reach 100% [5]. Initial reports of the disease date back to Montgomery's observations in Kenya in 1921 [6]. Presently, ASF has proliferated across Africa, Europe, and Asia, resulting in substantial economic and zootechnical ramifications [7].

In 2017, Romania reported its first case of ASF, identified in two domestic pigs in Satu Mare county, located in the northwest of the country. Subsequently, the disease surfaced in the Danube Delta, initially affecting domestic pigs and later confirmed in wild boars. The introduction of the virus was attributed to illicit trade in pork and pork products in Satu Mare and the migration of wild boars near the country's borders in the Danube Delta [8]. Since then, genotype II of ASFV has been identified in all counties of Romania [12]. Given Romania's substantial pork consumption and the significance of pig farming in the country's agriculture, the economic repercussions are keenly felt by households and large-scale industrial farms alike. Veterinary epidemiology plays a pivotal role in offering insights and guidance to regulatory agencies responsible for public health protection and animal health, particularly in understanding disease transmission trends within herds (SALMAN, 2009). External biosecurity risk factors have been identified as influential in the introduction and propagation of ASF within domestic pig herds, with numerous biosecurity-related factors playing a critical role in the dissemination and maintenance of ASF in domestic pig populations (VILTROP et al., 2021). Geoclimatic factors have also been demonstrated to impact the spread of ASFV (UNGUR et al., 2022).

The identification of new ASF outbreaks and prevention of its spread can be significantly facilitated through the examination of suspected clinical cases using rapid and sensitive laboratory methods [13]. Presently, real-time polymerase chain reaction (RT-PCR) stands as the most sensitive laboratory method for detecting ASFV, enabling the identification of viral DNA in tissues, blood, or serum even in the early stages of infection or advanced autolysis [14]. The various clinical forms of ASF infection, including peracute, acute, subacute, chronic, and subclinical, can be discerned through RT-PCR [14]. Supplementary laboratory methods, such as the detection of viral antigen, have proven highly sensitive for identifying acute ASFV infections, although their sensitivity diminishes in cases of subacute, chronic, or subclinical infection [13; 15; 16; 17]. Techniques such as the fluorescent antibody test (FAT), antigen-ELISA test, and immunohistochemistry can be employed for identifying ASFV antigens in tissue samples [13; 16].

The pathogenesis of ASF is characterized by vascular lesions and hemorrhages [18, 19; 20; 21; 22] and lymphoid depletion due to apoptosis of lymphocytes [16; 23]. Tonsils, as aggregates of lymph nodes and diffuse lymphoid tissues organized into independent lymphoid organs positioned at the junction of the nasopharynx and oropharynx, play a pivotal role in ASFV pathogenesis [24].

This study aimed to histologically evaluate the lesions induced by ASFV presence in the organism and contribute insights into the distribution and intensity of ASF viral antigen across various organs through immunohistochemical (IHC) examination. These methods enable the in-situ demonstration of viral protein, providing excellent visualization of cell and tissue morphology, primarily for use in pathogenesis and vaccine studies. Additionally, the IHC test can be employed for diagnostic purposes in acute cases of ASF if only formalin-fixed tissue samples are available for laboratory examination and for confirming RT-PCR results. The utility of Immunohistochemical Examination (IHC) for ASF diagnosis is reaffirmed, emphasizing the use of monoclonal antibodies to mitigate background staining. The study highlights robust immunostaining even in cases of tissue

 doi:10.20944/preprints202311.1487.v1

autolysis, underscoring the diagnostic resilience of this technique. The widespread distribution of the virus across organs, with tonsils as a consistent epicenter, underscores their crucial role in ASFV pathogenesis.

2. Materials and Methods

The biological material evaluated originated from 118 domestic pigs from all regions of the country, confirmed positive for African Swine Fever (ASF) by the Institute of Diagnostic and Animal Health (IDSA) through PCR examination, in the period 2018-2021. Tissue samples received, processed, and fixed in 10% neutral pH formalin were collected from lymph nodes, lungs, heart, tonsils, kidneys, spleen, liver, and gall bladder.

The histopathological examination was performed at the Department of Pathological Anatomy, Necropsy Diagnosis, and Veterinary Legal Medicine within the Faculty of Veterinary Medicine in Cluj-Napoca. For histological examination, the received samples were reprocessed to a thickness of 3mm and placed in special histological cassettes for embedding. The tissue cassette samples were then immersed in solutions of increasing concentrations of ethanol for dehydration. In the first ethanol bath with a concentration of 70%, the tissues were kept for one hour, followed by transfer to the second ethanol bath with a concentration of 95% for one hour, and finally to 100% ethanol for 4 hours, with the solution changed every hour. Throughout the 6-hour process, the ethanol baths were placed on a mechanical shaker. After dehydration, the samples were immersed in three xylene baths for clarification, changing the agent every hour. The next step involved immersing the samples in melted paraffin at 60°C for 2 hours. The subsequent stage included embedding the tissue samples in paraffin blocks and cooling them at -15°C for 30 minutes. The blocks were then sectioned at an approximate thickness of 2 microns using the Thermo Scientific™ HM 325 manual microtome.

2.1. Histology

The obtained tissue sections were spread on plain histological slides and kept in an incubator at a temperature of 37°C for 4 hours to ensure effective tissue adhesion, and then manually stained with hematoxylin and eosin (H&E). For each organ, a lesion evaluation protocol was established, and the lesions were classified. At the level of the kidneys, the presence or absence of parenchymal hemorrhages, interstitial inflammation, renal epithelial cell necrosis, vasculitis lesions, microthromboses, and hydropic degeneration were noted. To assess the intensity of hemorrhages, edema, inflammatory, and necrotic lesions, a scoring system described in the literature [25] was used. Four microscopic fields were examined for each sample using a low-power objective (5x). Depending on the area occupied by the studied lesions, the following scores were assigned: absence of lesions (-); 0-20% (+); 20-50% (++); >50% (+++). For liver sections, the severity of hemorrhages, parenchymal inflammation, and hepatocellular necrosis was evaluated, followed by noting the presence or absence of vasculitis lesions and microthromboses. At the gall bladder level, the protocol involved evaluating wall edema, interstitial hemorrhage degree, and epithelial necrosis, and noting the presence or absence of vasculitis lesions and microthromboses. In the case of spleen preparations, the severity of parenchymal hemorrhages, interstitial inflammation, and necrosis was assessed, along with the presence or absence of vasculitis lesions and microthromboses. Lymph node preparations were categorized based on the severity of interstitial hemorrhages and lymphoid depletion, as well as the presence or absence of vasculitis lesions and microthromboses. For myocardial tissue, the presence or absence of interstitial edema, interstitial hemorrhages, myocyte necrosis, and the presence or absence of vasculitis lesions and microthromboses were noted. Lungs were examined to determine the presence of edema, alveolar congestion, hemorrhages, necrosis, and interstitial inflammation. For intestine sections, inflammatory and necrotic lesions were evaluated, along with the severity of hemorrhages, followed by noting the presence or absence of edema and vasculitis lesions, as well as microthromboses.

 doi:10.20944/preprints202311.1487.v1

2.2. Immunohistochemistry (IHC)

The obtained tissue sections were spread on special histological slides treated with polylysine and then kept in an incubator at a temperature of 37°C for 12 hours to ensure adhesion and prevent tissue detachment from the slide. The process continued with deparaffinization of the spread samples using xylene and their rehydration in successive baths of increasing concentrations of ethanol, followed by immersion in distilled water. The next step involved blocking endogenous peroxidase activity by incubating the sections in a 3% hydrogen peroxide solution - methanol, produced by Novocastra, for 10 minutes at 24°C and washing with phosphate-buffered saline (PBS). Antigenic demasking was enzymatic, using a commercial kit produced by Leica, by incubating the sections at a temperature of 37°C for 10 minutes, followed by washing with PBS. After washing, a protein blocking solution produced by Novocastra was applied for 15 minutes at room temperature to prevent background coloration. Following this step, the sections were incubated with primary mouse monoclonal antibodies against p72 (clone 1BC11, Ingenasa) in a diluted solution of 1:2000, and the sample was left at room temperature for 4 hours. Subsequently, the Novocastra universal secondary antibody solution was applied for one hour at room temperature. After two consecutive washes with PBS, the secondary antibody was applied. After washing, the Novolink polymer reagent was applied and left to act for 15 minutes. For immunomarking reaction visualization, a 3-3' diaminobenzidine chromogen solution was applied at a dilution of 1:20 for 20 minutes. Finally, the tissues were dehydrated in successive baths of ethanol solutions (70%, 96%, and 100%) for 5 minutes, and then clarified in two xylene baths for 10 minutes each. Counterstaining of the samples was performed using Mayer's hematoxylin solution to observe the site of immunoreaction. The immune reaction was considered positive when the cytoplasm or membrane of cells infected with ASF virus showed varying shades of brown staining.

Microscopic examination of the samples and digital image capture were performed using a system for capturing, processing, and retrieving microscopic images, consisting of a Zeiss Scope.A1 optical microscope connected to a Zeiss Axiocam 208 color digital camera. Image retrieval and processing were carried out using the specialized ZEISS ZEN core v3.0 software.

3. Results

3.1. Histology

Histological examination was conducted on all received samples. Approximately one-quarter of them were well-preserved and ideal for microscopic diagnosis. However, 13 samples could not be examined due to advanced autolysis. Most samples showed varying degrees of autolysis, but examination was possible since tissue morphology remained intact, and most cellular borders could be recognized, even though most cells lacked nuclear staining. Cells resembling macrophages and lymphocytes mostly had intact nuclei. Characteristic tissue lesions for acute ASF were detected in the majority of samples. Severe hyperemia or hemorrhages that distorted tissue morphology and caused cell lysis were evident in a significant number of samples.

Multifocal acute hemorrhages were particularly prominent in the heart, lungs, kidneys, liver, and spleen. Severe and diffuse hyperemia along with acute hemorrhage was observed in lymph nodes. Diffuse lymphoid depletion characterized by a variable prevalence of lysis and lymphocyte loss was present in the spleen and lymph nodes. An inflammatory infiltrate, mainly composed of monocytes with only a few neutrophils and eosinophils, ranging from mild to moderate severity, was observed in the heart, lungs, liver, and kidneys.

One or more types of vascular lesions were observed in each examined organ: endothelial cell activation, intramural edema, fibrinoid necrosis of vascular walls, vasculitis/perivasculitis, and the presence of intravascular thrombi.

In the lungs, additional tissue lesions included acute necrotic bronchiolitis, severe interlobular edema along with inflammatory infiltrate, and varying amounts of fibrin in the alveolar lumen. In the kidneys, severe acute tubulonephrosis was observed, characterized by extensive areas of tubular necrosis and multifocal tubule dilation. The main histopathological changes in the tonsils were

 doi:10.20944/preprints202311.1487.v1

lymphoid depletion in lymphoid follicles and interfollicular interstitium, along with vascular changes such as hemorrhage and congestion.

3.1.1. Kidney

Among the 118 received renal tissue samples, 114 underwent study due to advanced autolysis in 4. Parenchymal hemorrhages were detected in 100 samples (87.7%), while microthromboses were found in 58 samples (50.8%) within the cohort. Vasculitis lesions manifested in a limited 36 samples (31.5%), juxtaposed with renal parenchymal inflammation observed in 62 samples (54.3%). Necrotic regions appeared in 47 samples (41.2%), and hydropic degeneration was noted in 100 samples (87.7%) with varying degrees of severity.

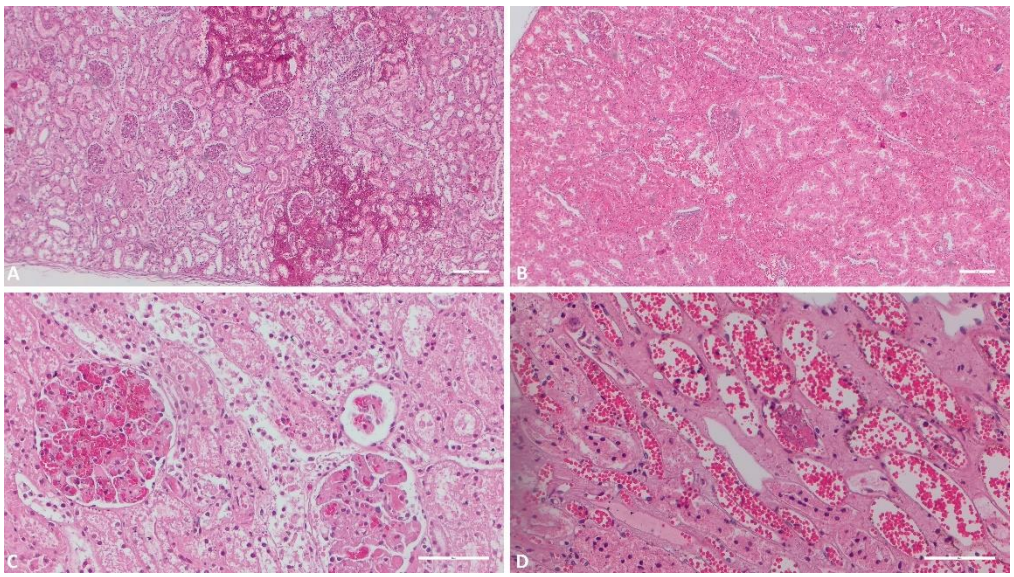

Figure 1. Histologic evaluation of the kidneys. A) (Scale at 50μm) Multiple foci of interstitial hemorrhage; B) (Scale at 50μm) Severe congestion, interstitial hemorrhage; C) (Scale at 100μm) Glomerular hemorrhage, hydropic degeneration of the epithelial renal cells of the tubuli; D) (Scale at 100μm) Severe congestion, necrosis of the epithelial renal cells, vascular micro thrombi.

3.1.2. Liver

Out of the total 118, only one liver sample was compromised by advanced autolysis, leaving 117 for further examination. Parenchymal hemorrhages manifested in 42 samples (35.8%), while necrotic lesions presented in 21 samples (17.9%). Varied degrees of inflammation were apparent in 37 samples (31.6%). Microthromboses occurred in a scant 2 out of 117 samples (1.7%).

Preprints (www.preprints.org) | NOT PEER-REVIEWED | Posted: 23 November 2023 doi:10.20944/preprints202311.1487.v1

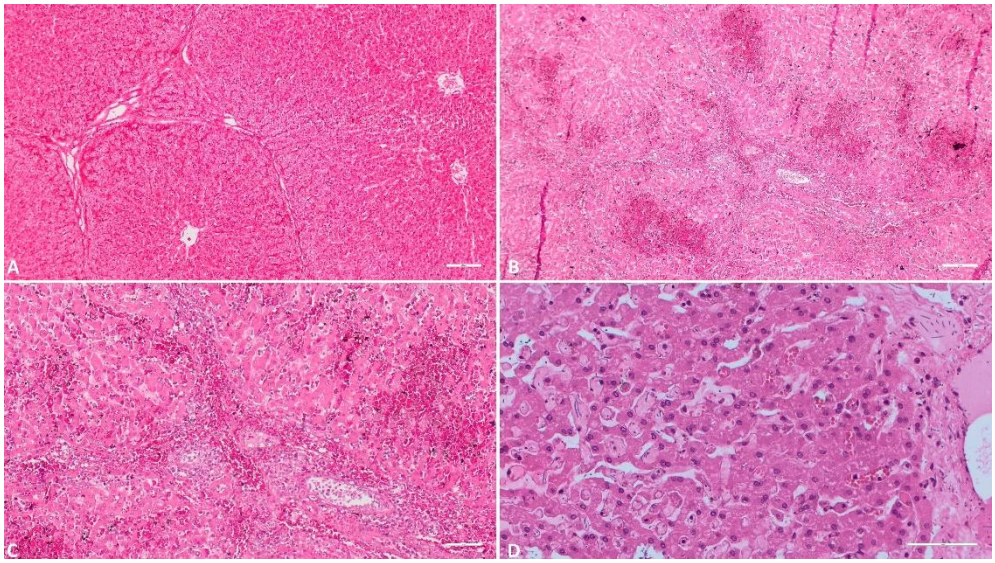

Figure 2. Histologic evaluation of the liver. A) (Scale at 50μm) Severe congestion of the sinusoid capillaries; B) (Scale at 50μm) Multiple foci of hemorrhage in the inter and intra lobular areas; C) (Scale at 100μm) Massive hemorrhage in the hepatic parenchyma; inflammatory infiltrate; D) (Scale at 50μm) Congestion of sinusoid capillaries, necrosis of hepatocytes, interstitial edema.

3.1.3. Gallbladder

Of the 118 gallbladder samples, one proved unsuitable for histological inquiry. Among the remaining specimens, severe gallbladder edema was present in 60 samples (51.3%), moderate edema in 28 (23.9%), incipient edema in 3 (2.6%), and 26 samples (22.2%) exhibited no edematous signs. Hemorrhagic lesions characterized 58 samples (49.5%), while 18 samples (15.3%) displayed necrotic features.

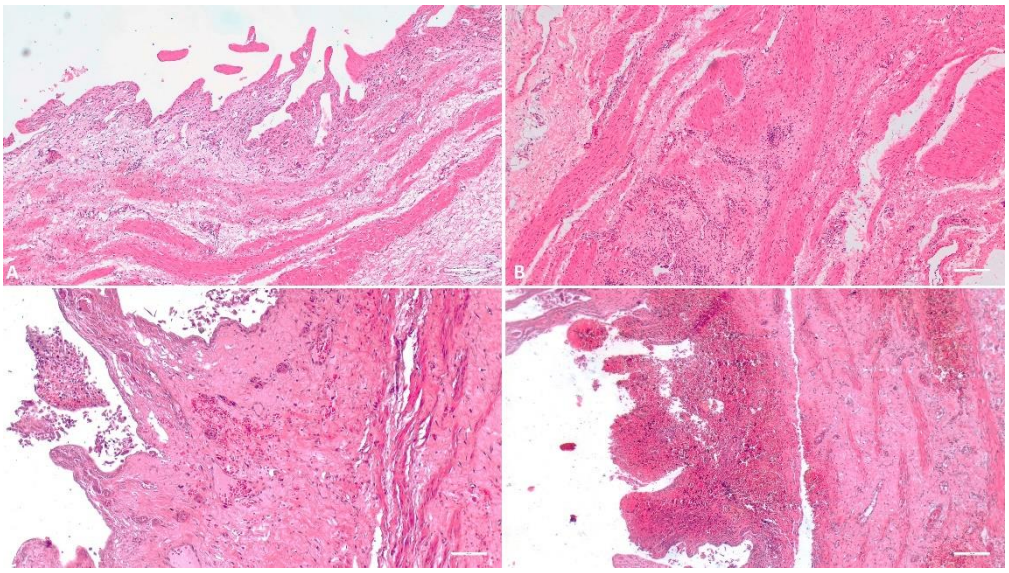

Figure 3. Histologic evaluation of the gallbladder. A) (Scale at 50μm) Thickening and edema of the gallbladder wall; B) (Scale at 50μm) Edema, inflammatory infiltrate; C) (Scale at 50μm) Interstitial hemorrhage of the wall, necrosis of the epithelial cells, inflammatory infiltrate; D) (Scale at 50μm) Severe hemorrhage.

Preprints (www.preprints.org) | NOT PEER-REVIEWED | Posted: 23 November 2023 doi:10.20944/preprints202311.1487.v1

3.1.4. Spleen

Two out of the 118 received spleen tissue samples suffered advanced autolysis, reducing the study size to 117. Among these, 31 samples (26.7%) displayed various degrees of parenchymal inflammation. Hemorrhagic lesions were present in 108 samples (93.1%), while necrotic lesions and lymphoid depletion appeared in 79 samples (68.1%). Splenic microthromboses were identified in 28 samples (24.1%).

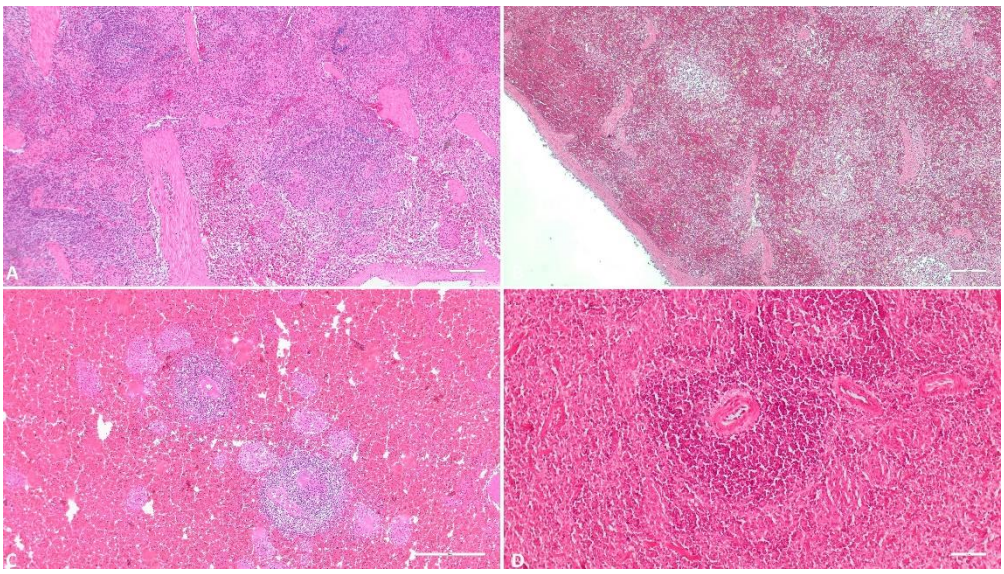

Figure 4. Histologic evaluation of the spleen. A) (Scale at 50µm) Multiple foci of interstitial hemorrhage and congestion, spleen architecture suffers mild changes; B) (Scale at 50µm) Medium degree of parenchymatous hemorrhage, several foci of lymphoid depletion, spleen architecture suffers medium changes; C) (Scale at 50µm) Massive parenchymatous hemorrhage, diffuse necrosis, spleen architecture severely affected; D) (Scale at 100µm) Massive parenchymatous hemorrhage, diffuse necrosis, perivasculitis.

3.1.5. Lymph Node

From the total of 118 received lymph node tissue samples, one failed histopathological assessment. Of the remaining samples, 98 (83.7%) exhibited hemorrhagic lesions of diverse intensity. Necrotic features appeared in 72 samples (61.5%). Perivascular infiltrate was evident in 14 samples (11.9%), and microthromboses were noted in 67 samples (57.2%).

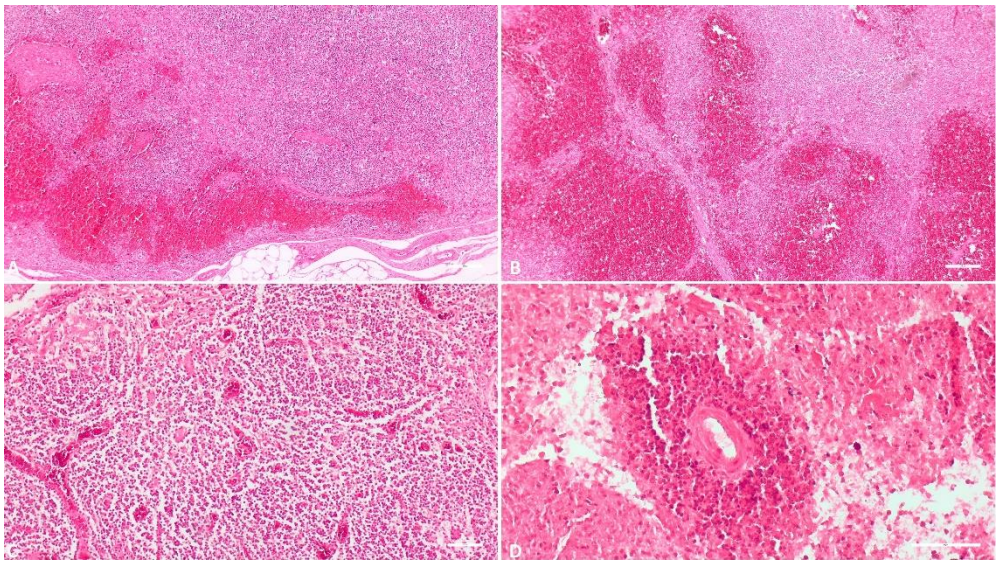

 doi:10.20944/preprints202311.1487.v1

Figure 5. Histologic evaluation of the lymph nodes. A) (Scale at 50µm) Cortical and subcapsular hemorrhage, medullar congestion; B) (Scale at 50µm) Severe cortical hemorrhage, medullar congestion and mild hemorrhages; C) (Scale at 100µm) Congestion, vascular micro thrombi, diffuse necrosis; D) (Scale at 100µm) Hemorrhage, diffuse necrosis, perivasculitis.

3.1.6. Heart

One of the 118 received heart tissue samples was unsuitable for histopathological examination due to advanced postmortem changes. Hence, the study encompassed 117 heart tissue samples. Within this group, 54 samples (46.1%) displayed subepiendocardial, myocardial, or subendocardial hemorrhages of varying severity. Necrotic features were present in 12 samples (10.2%). Different degrees of myocardial edema were apparent in 81 samples (69.2%), with 65 in an incipient stage. An ancillary observation, of marginal relevance to this study yet noteworthy, was the identification of cystic forms of Sarcocystis spp. in 17 samples (14.5%) of those examined.

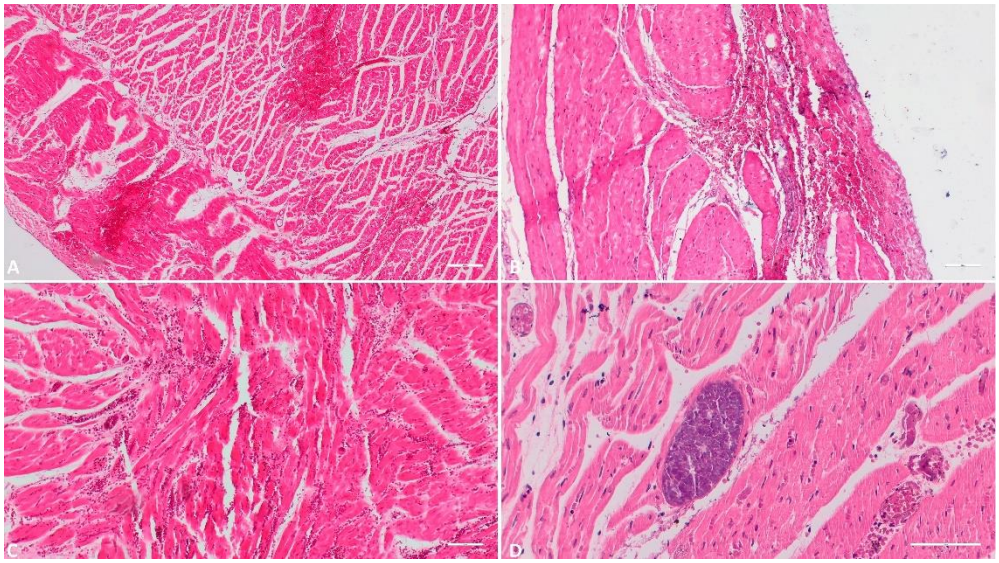

Figure 6. Histologic evaluation of the heart. A) (Scale at 50µm) Epicardial hemorrhage, myocardial edema and hemorrhage; B) (Scale at 50µm) Endocardial foci of hemorrhage and necrosis; C) (Scale at 50µm) Myocardial hemorrhage and necrotic foci; D) (Scale at 100µm) Parasitic cyst of Sarcocystis spp.

3.1.7. Lung

Regarding the received lung tissue samples, all 118 were deemed suitable for histological examination. Pulmonary interstitial congestion was universal, observed in 100% of samples, with varying degrees of severity: 77 samples (65.2%) exhibited mild congestion, 22 samples (18.7%) displayed moderate congestion, and 19 samples (16.1%) showcased severe congestion. Pulmonary edema was identified in 82 of the samples (69.4%), with 34 (28.8%) exhibiting hemorrhagic lesions and 18 (15.2%) displaying varying degrees of necrosis. Interstitial pneumonia was detected in 62 samples (52.5%) within the total, while thrombus formation was noted in 26 samples (22.0%).

Preprints (www.preprints.org) | NOT PEER-REVIEWED | Posted: 23 November 2023 doi:10.20944/preprints202311.1487.v1

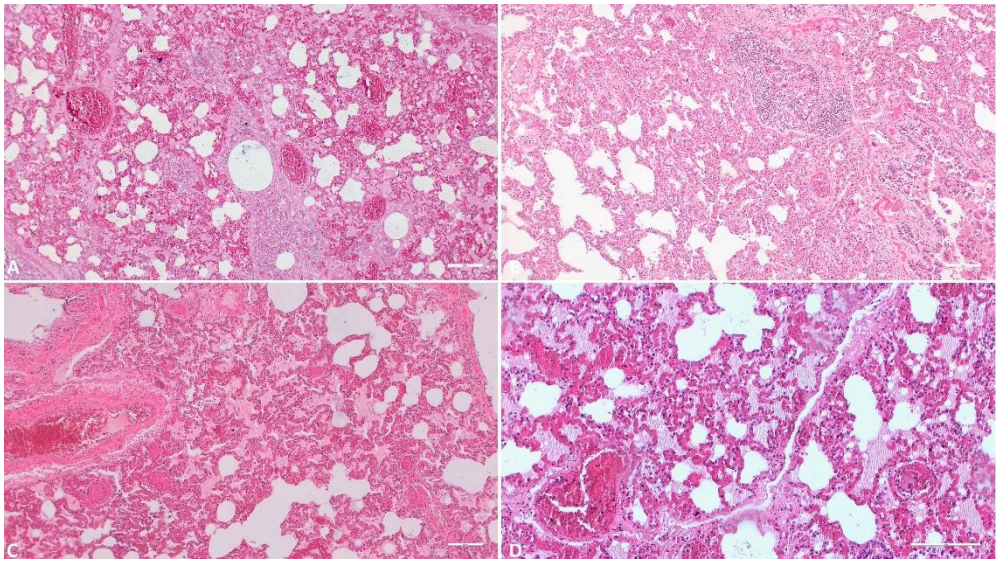

Figure 7. Histologic evaluation of the lungs. A) (Scale at 50µm) Alveolar wall thickening, sever congestion, alveolar edema; B) (Scale at 50µm) Massive hyperplasia of the lung interstitium, inflammatory infiltrate, hyperplasia of the bronchiolar associated lymphoid tissue; areas of alveolar emphysema; C) (Scale at 50µm) Severe pulmonary congestion and edema; D) (Scale at 50µm) Severe alveolar edema, alveolar wall congestion, vascular micro thrombi.

3.1.8. Tonsil

Among the tonsil samples, three underwent advanced postmortem changes, necessitating the study to be conducted on 115 samples. The most prominent alteration was congestion, which was evident in 101 of the samples (87.8%). Hemorrhagic lesions of diverse severity were present in 27 samples (23.4%), and necrotic features, including lymphoid depletion, were observed in 62 samples (53.9%). Thrombus formation was noted in 17 samples (14.7%).

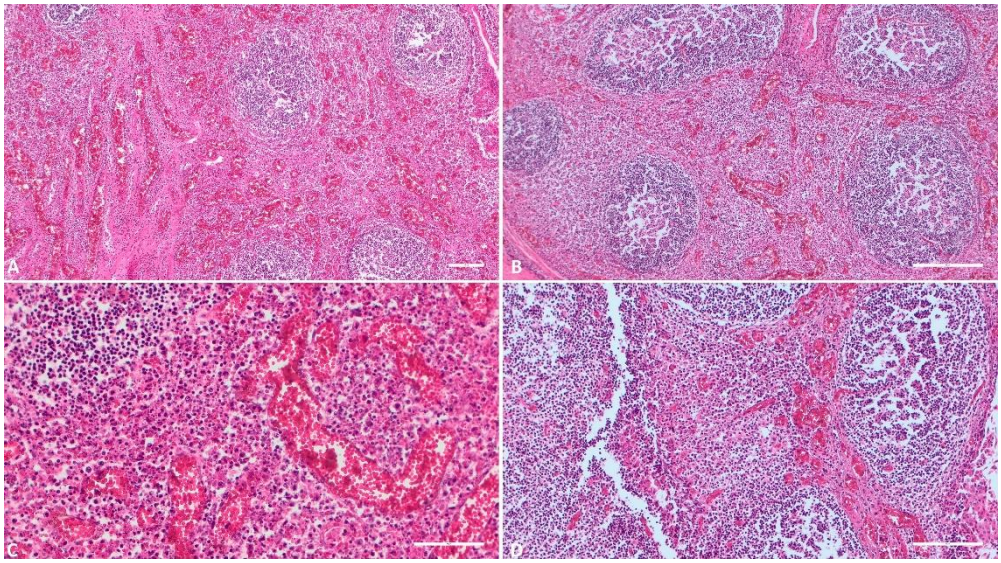

Figure 8. Histologic evaluation of the tonsils. A) (Scale at 50µm) Severe interstitial congestion and hemorrhage; B) (Scale at 100µm) Interstitial congestion, lymphoid depletion; C) (Scale at 100µm) Congestion, vascular micro thrombi, connective tissue proliferation; D) (Scale at 50µm) Congestion, hemorrhage, necrosis, cellular fragmentation, inflammatory infiltrate.

 doi:10.20944/preprints202311.1487.v1

3.2. IHC

The major p72 protein from the PPA virus capsid was detected in a significant portion of the examined tissue samples. The highest number of positive vPPA samples, 107 out of 118 (90.6%), were identified in the tonsils. Positive immunolabeling was also found in 98 (83.0%) samples from kidneys and lymph nodes. In other organs, the presence of the virus was confirmed as follows: gallbladder 93 samples (78.8%), spleen 79 samples (66.9%), heart 67 samples (56.7%), lungs 61 samples (51.69%), liver 54 samples (45.7%), and intestines 26 samples (22.0%).

In some cases, due to autolysis, the characterization of infected cell types was not feasible. A moderate to high number of macrophage-like cells were immunolabeled in most of the examined tissue samples. Three types of immunostaining patterns were observed within the cytoplasm of infected cells: granular (resembling inclusions) or diffuse (with varying intensities). Diffuse immunolabeling was so intense in some cells that it occasionally obscured their nuclei (Figure 9C). In a few cells, the inclusion-like immunostaining was so strong that it entirely covered the cell nucleus, closely resembling nuclear immunostaining (Figure 9C). The major capsid protein p72 was also detected extracellularly in the form of fine to coarse granular immunostaining both in areas of tissue affected by cariorhexis and in the lumen of the vascular system (Figure 9D, 10A, C, 11B, D). Slight diffuse background staining was observed in many of the examined samples. No immunostaining was detected in tissue samples from the negative control batches.

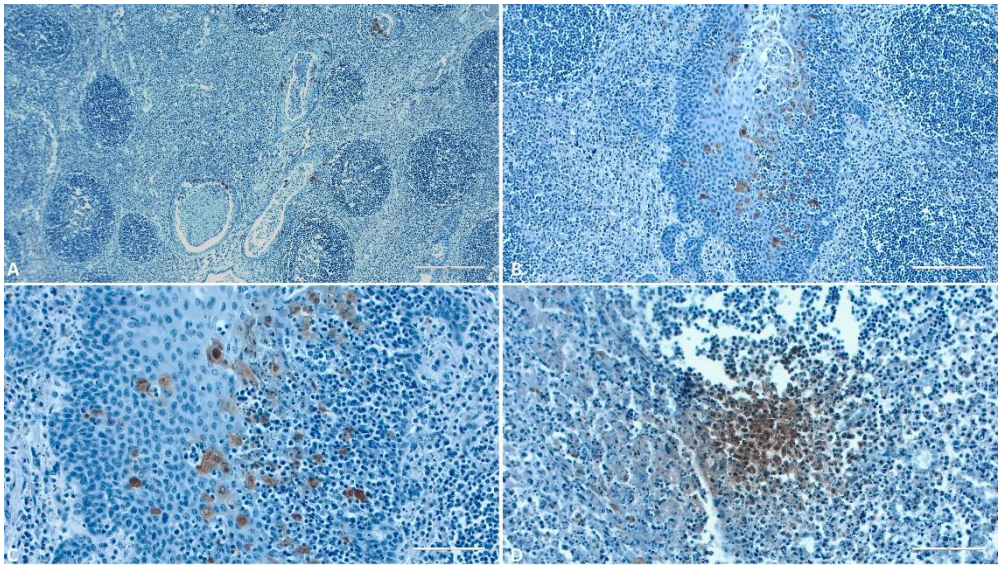

Figure 9. IHC evaluation of the tonsils. A) (Scale at 25µm) Positive reaction in the endothelial cells, circulating monocytes and of several macrophages from the interstitial space; B-C) (Scale at 50µm [B], 100µm [C]) Monocytes and macrophages with positive reaction inside a tonsillar crypt with different staining patterns.; D) (Scale at 100µm) Strong positive reaction in monocytes from the interstitial space, diffuse background granular staining.

Within this study, immunolabeling reactions were notably more numerous and evident in the tonsils. The highest number of immunolabeled macrophage-like cells was observed in all structures of these organs (Figure 9). Their abundance was particularly pronounced in the lymphoid follicles (Figure 9 B, C). The major capsid protein p72 was found in the interfollicular interstitium (Figure 9 A) and in the perifollicular lymphoid tissues, with only a few epithelial cells exhibiting a positive reaction.

Preprints (www.preprints.org) | NOT PEER-REVIEWED | Posted: 23 November 2023 doi:10.20944/preprints202311.1487.v1

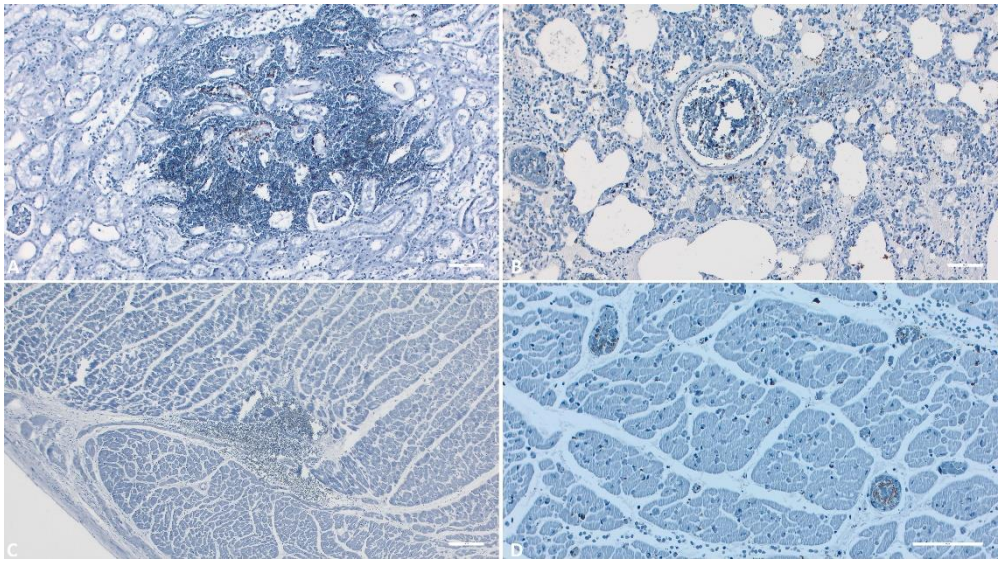

Figure 10. IHC evaluation of the kidneys, lungs and heart. A) Kidney (Scale at 50µm) – Positive reaction in the interstitial hemorrhage area; B) Lungs (Scale at 50µm) – positive reaction of the macrophages and dendritic cells; C) Heart (Scale at 100µm)– Positive reaction in the interstitial hemorrhage area; D) Heart (Scale at 50µm)– Positive reaction of the endothelial cells and circulating monocytes.

Within the heart, lungs, and kidneys, the most intensely positive immunoreaction areas were observed in the blood vessels (Figure 11 B, D), coinciding with areas of hemorrhage (Figure 11 A, C). The major capsid protein p72 was detected multifocally in the majority of monocytes within these organs, as well as in some dendritic cells in the lungs (Figure 11 B). A granular background staining was observed in the majority of examined organs.

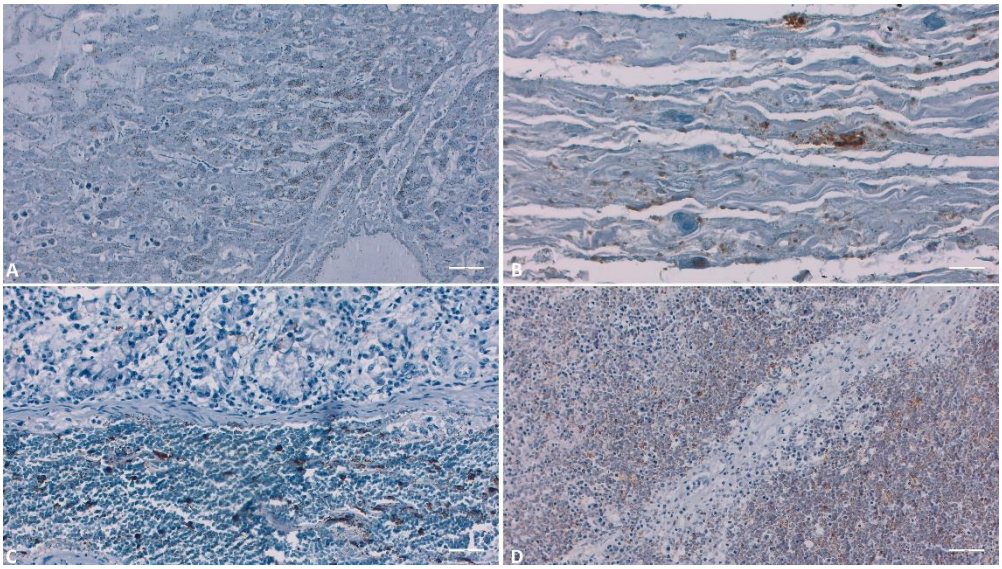

Figure 11. IHC evaluation of the liver, gallbladder, intestine and lymph nodes. A) Liver (Scale at 100µm) – Positive reaction of the Kupfer cells and hepatocytes; B) Gallbladder (Scale at 100µm) – Positive reaction in the hemorrhagical areas; C) (Scale at 100µm) – Positive reaction in the hemorrhagical areas; D) Lymph nodes (Scale at 50µm) – Strong positive reaction in the hemorrhagical areas.

In the case of liver samples, IHC demonstrated the presence of p72, particularly in the cells lining the sinusoidal spaces, such as Kupffer or endothelial cells, as well as in a small number of hepatocytes (Figure 12A). Upon examining the gallbladder, both the hemorrhagic areas and the epithelial regions

 doi:10.20944/preprints202311.1487.v1

showed intense labeling (Figure 12B). In the tissues of the liver, gallbladder, and intestines (Figure 12C), a substantial number of positive monocytes were observed within the lumens of blood vessels. In lymph nodes and the spleen, immunohistochemical analysis highlighted cytoplasmic immunoreactivity in macrophages and monocytes. The immunostaining pattern was either diffuse or inclusion-like. Hemorrhagic areas as well as blood vessels exhibited the most intense reactivity (Figure 12 D).

4. Discussion

4.1. Histology

In the context of our study, a comprehensive histopathological investigation was undertaken on samples obtained from both domestic swine and European wild boars. The observed pathological findings substantiate the characteristic immunosuppression associated with acute African Swine Fever (ASF) infection [26]. Notably, lymphoid depletion, a consequence of lymphocyte apoptosis, a phenomenon well-documented in the literature [27; 16], particularly in lymphoid organs such as the spleen [23], lymph nodes [20], and tonsils [28], was a consistent histopathological observation in our study.

Consistent with analogous investigations, vascular anomalies giving rise to hemorrhagic events were prominently conspicuous in the microscopic realm. These vascular alterations were pervasive across nearly all organs examined, including the spleen [29; 30], kidneys [31; 32; 33; 30], and lymph nodes [31; 32; 33; 30;34]. Subsequent to vascular alterations, a considerable proportion of the study cohort exhibited alveolar edema, a finding consistently echoed in similar inquiries [31; 25;34]. Intriguingly, the involvement of gallbladder wall edema, a phenomenon not commonly featured in recent literature, was also discernible.

In congruence with prior research, our study discerned vascular perturbations, notably vasculitis or perivasculitis, predominantly within the kidneys and lymph nodes. However, juxtaposed with precedent studies, the manifestation of these vascular lesions was not observed within the liver [29;34] and lungs [25]. This investigation also departed from the conventional by omitting certain organs from scrutiny, including intestines [34], bone marrow [34], and testicles and epididymis [31], thereby deviating from broader investigation trends.

Moreover, the study revealed an increased prevalence of microthromboses in lymph nodes, kidneys, and lungs, mirroring findings in the extant literature [34]. Nevertheless, in the liver [31], the incidence of microthromboses appeared subdued. Additionally, necrotic lesions were a distinctive histopathological hallmark, albeit their incidence exhibited variegated distribution across the evaluated organs. Specifically, pronounced prevalence of necrotic lesions was notable in samples derived from lymphoid tissues of the spleen [29; 25; 32;34], lymph nodes [30; 32;34], and tonsils [31; 32;34]. Conversely, the liver [25; 33] and kidneys [31; 33;34] exhibited a less pronounced frequency of such necrotic manifestations. The present study notably refrained from scrutinizing certain organs, including intestines [34], attributes which have been delineated in the literature.

Concomitantly, the study spotlighted another dimension of pathology, namely inflammatory lesions within the kidneys, typified by a lymphoplasmacytic inflammatory infiltrate localized in the renal cortex, a feature consonant with earlier studies [32;34]. Akin to prior investigations, the presence of inflammatory lesions was also discerned within the tonsils [31], heart [30], and liver, characterized by an inflammatory infiltrate encompassing periportal areas and comprising macrophages, lymphocytes, and occasionally plasma cells, a motif also echoed in the literature [32;34]. Furthermore, this study recognized the emergence of inflammatory infiltrates inclusive of granular cells within the lungs [31; 25] and lymph nodes [34]. Although analogous studies have outlined inflammatory lesions within organs such as testicles and epididymis [31], brain [31; 30], or intestines [34], these domains were not investigated in the current study.

IHC

The utility of Immunohistochemical Examination (IHC) for diagnosing African Swine Fever (ASF), utilizing both monoclonal and polyclonal antibodies, has been elucidated in antecedent

 doi:10.20944/preprints202311.1487.v1

studies [35; 17; 16; 28; 37]. In a seminal investigation, multiple tissue samples from naturally infected pigs were subjected to IHC analysis [17]. Among individuals with acute or subacute disease forms, all 11 (100%) demonstrated affirmative IHC results, while among those with chronic manifestation, 11 (69%) displayed positivity in one or more tissue samples. These outcomes, coupled with our findings, underscore the efficacy of immediate 10% formalin fixation post-tissue collection in averting tissue degradation, thus preserving intact capsid proteins of the ASF virus for supplemental antigen detection approaches, such as IHC.

Given the intense background staining associated with porcine-derived polyclonal antibodies, the recourse to monoclonal antibodies has been advocated within IHC testing [17; 37]. Our results buttress this recommendation, elucidating minimal background staining with negligible intensity, confined exclusively to areas afflicted by necrosis. Prior investigations have employed undiluted monoclonal antibodies specific to the ASF virus, with an incubation period of 30 minutes at room temperature [16], or diluted 1:10 and incubated overnight at 4°C [36; 28]. The protocol emulated in our study aligned with a contemporary inquiry [37], proving superior by mitigating spurious signals and resource expenditure through a high dilution of 1:2000. The untested anti-p72 Mab 1BC11 clone, introduced in Romania, demonstrated robust immunostaining when used in tandem with a specifically labeled polymer-based kit at this dilution. Moreover, this methodology enabled the identification of ASF virus even within tissue samples displaying advanced autolysis. All reagents employed in this investigation are commercially procurable, rendering the protocol facile for replication across appropriately equipped laboratories.

The merits of this technique rest in the ASF virus inactivation by formaldehyde, while preserving viral antigens in a stable configuration [37]. Formalin-fixed, paraffin-embedded tissue specimens are optimal substrates for retrospective investigations into ASF using IHC [38]. However, certain constraints circumscribe its routine diagnostic applicability, manifesting as time-intensive and unsuitable for surveillance assays, recommended primarily for acute ASF cases [37].

Drawing from prior studies, the major capsid protein of the ASF virus has evinced multifarious cellular detection, contingent upon the disease's clinical expression and the implicated viral strain's pathogenicity [35; 17, 36; 16; 28]. Mononuclear phagocytic cells emerge as the chief targets of ASF infection, while later disease stages encompass other cell varieties, including hepatocytes, neutrophils, epithelial cells, and endothelial cells [17; 36]. The incipient clinical stage of ASF among our subjects may account for the exclusive immunolabeling of macrophages and sparse endothelial cells. The established immunostaining pattern aligns with earlier accounts, characterized by either diffuse or intracellular inclusion-like staining [17; 36; 16; 37]. Notably, the present study unveils a granular immunostaining pattern in the cytoplasm of infected cells. A recent study [37] outlined extracellular immunostaining in pulmonary tissues, primarily within necrotic zones and the vascular lumen. These features coalesced within our inquiry, manifesting across lymphoid organs (tonsils and lymph nodes), and encompassing the heart, kidneys, and gallbladder. Noteworthy extracellular viral particles of ASF have been alluded to in extant studies [20; 27, 34; 38], albeit in summary fashion.

5. Conclusions

In conclusion, this study represents a pioneering endeavor in the comprehensive elucidation of histopathological alterations encountered in African Swine Fever (ASF), encompassing a cohort of over 100 confirmed positive porcine subjects. Our investigation has spotlighted the lymph nodes, spleen, and kidneys as the pivotal organs susceptible to the manifestations of African Swine Fever Virus (ASFV). Primarily, vascular involvement coupled with ensuing consequential lesions emerged as the predominant histopathological variations. Notably, hemorrhagic manifestations assumed prominence in the spleen (93.1%), kidneys (87.7%), and lymph nodes (83.7%), underscoring the virus's predilection for these regions. Moreover, a noteworthy prevalence of necrotic lesions was evident in the spleen (68.1%), lymph nodes (61.5%), and tonsils (53.9%). Importantly, our findings reveal a marked prevalence of microthromboses, notably conspicuous in the lymph nodes (57.2%) and kidneys (50.8%). Intriguingly, the presence of tissue sample autolysis does not appear to compromise the sensitivity of the IHC assay, rendering it a robust diagnostic tool. Our investigation

further underscores that the viral presence was discerned across all examined organs, with circulating monocyte populations, tissue-resident macrophages, and endothelial cells of small vessels being the primary cellular enclaves harboring the viral antigen. The distinct prominence of antigen-positive cells in tonsils, kidneys, and lymph nodes underscores their critical role in viral dissemination. Notably, tonsils emerged as the consistent epicenter of viral presence across all cases examined, with the intensity of immunostaining in tonsils exceeding that in other tissue specimens. Collectively, these findings corroborate the virus's initial preferential propagation at this anatomical locus, shedding light on the intricate pathogenesis of ASFV.

Author Contributions: Conceptualization, A.U. and A.N.; methodology, A.U..; software, A.U..; validation, A.N.., and C.C..; formal analysis, A.U..; investigation, A.U..; resources, A.U. and C.C..; data curation, A.U.; writing—original draft preparation, A.U..; writing—review and editing, C.C..; visualization, A.U..; supervision, C.C..; project administration, A.U..; funding acquisition, C.C. All authors have read and agreed to the published version of the manuscript.

Funding: "This research received no external funding.

Data Availability Statement: "Not applicable".

Acknowledgments: Romanian National Institute for Veterinary Diagnosis (IDSA) provided all the biological material used in this study.

Conflicts of Interest: The authors declare no conflict of interest.

References

1. BERGMANN, H.; SCHULZ, K.; CONRATHS, F.J.; SAUTER-LOUIS, C., 2021. A Review of Environmental Risk Factors for African Swine Fever in European Wild Boar. Animals, 11, 2692.
2. MAZUR-PANASIUK, N., ŻMUDZKI, J., & WOŹNIAKOWSKI, G., 2019. African swine fever virus – persistence in different environmental conditions and the possibility of its indirect transmission. Journal of Veterinary Research, 63(3), 303-310.
3. BLOME, S., FRANZKE, K., & BEER, M., 2020. African swine fever – A review of current knowledge. Virus Research, 287, 198099.
4. FISCHER, M.; HÜHR, J.; BLOME, S.; CONRATHS, F.J.; PROBST, C., 2020. Stability of African Swine Fever Virus in Carcasses of Domestic Pigs and Wild Boar Experimentally Infected with the ASFV "Estonia 2014" Isolate. Viruses, 12, 1118.
5. BELLINI, S.; CASADEI, G.; DE LORENZI, G.; TAMBA, M., 2021. A Review of Risk Factors of African Swine Fever Incursion in Pig Farming within the European Union Scenario. Pathogens, 10, 84.
6. MONTGOMERY, R.E., 1921. On A Form of Swine Fever Occurring in British East Africa (Kenya Colony). J. Comp. Pathol. Ther., 34, 159–191.
7. SAUTER-LOUIS, C.; CONRATHS, F.J.; PROBST, C.; BLOHM, U.; SCHULZ, K.; SEHL, J.; FISCHER, M.; FORTH, J.H.; ZANI, L.; DEPNER, K.; ET AL., 2021. African Swine Fever in Wild Boar in Europe—A Review. Viruses, 13, 1717
8. BOKLUND, A.; CAY, B.; DEPNER, K.; FÖLDI, Z.; GUBERTI, V.; MASIULIS, M.; MITEVA, A.; MORE, S.; OLSEVSKIS, E.; ŠATRÁN, P.; ET AL., 2018. Epidemiological analyses of African swine fever in the European Union (November 2017 until November 2018). EFSA J., 16, e05494.
9. Ungur, A.; Cazan, C.D.; Panait, L.C.; Taulescu, M.; Balmoș, O.M.; Mihaiu, M.; Bărbuceanu, F.; Mihalca, A.D.; Cătoi, C. Genotyping of African Swine Fever Virus (ASFV) Isolates in Romania with the First Report of Genotype II in Symptomatic Pigs. Vet. Sci. 2021, 8, 290. https://doi.org/10.3390/vetsci8120290
10. SALMAN, M., 2009. The role of veterinary epidemiology in combating infectious animal diseases on a global scale: The impact of training and outreach programs. Prev. Vet. Med., 92, 284–287.
11. VILTROP, A.; REIMUS, K.; NIINE, T.; MÕTUS, K., 2021. Biosecurity Levels and Farm Characteristics of African Swine Fever Outbreak and Unaffected Farms in Estonia—What Can Be Learned from Them? Animals, 12, 68.
12. Ungur, A.; Cazan, C.D.; Panait, L.-C.; Coroian, M.; Cătoi, C. What Is the Real Influence of Climatic and Environmental Factors in the Outbreaks of African Swine Fever? Animals 2022, 12, 781. https://doi.org/10.3390/ani12060781
13. GALLARDO, M.C., REOYO, A.D.L.T., FERNÁNDEZ-PINERO, J. ET AL., 2015. African swine fever: a global view of the current challenge. Porc Health Manag 1, 21.

14. OURA C.A.L., L. EDWARDS, C.A. BATTEN., 2013. Virological diagnosis of African swine fever—Comparative study of available tests, Virus Research 1., 173., 150-158,.
15. GALLARDO, C., FERNÁNDEZ-PINERO, J., & ARIAS, M., 2019. African swine fever (ASF) diagnosis, an essential tool in the epidemiological investigation. Virus Research, 271, 197676
16. OURA CA, POWELL PP, PARKHOUSE RM., 1998. African swine fever: a disease characterized by apoptosis. J Gen Virol. 79 (Pt 6):1427–38.
17. PÉREZ, J., RODRÍGUEZ, F., FERNÁNDEZ, A., DE LAS MULAS, J.M., GÓMEZ-VILLAMANDOS, J.C., SIERRA, M.A., 1994. Detection of African swine fever virus protein VP73 in tissues of experimentally and naturally infected pigs. J. Vet. Diagn. Invest. 6, 360–365.
18. MOULTON J. E., PAN I. C., HESS W. R., DEBOER C. J., TESSLER J., 1975. Pathologic features of chronic pneumonia in pigs with experimentally induced African swine fever. American Journal of Veterinary Research 36(1):27-32.
19. RUIZ-GONZALVO F., CARNERO M.E., BRUYEL V., 1981. Immunological responses of pigs to partially attenuated African swine fever virus and their resistance to virulent homologous and heterologous viruses. Wilkinson P.J., pp. 206–216.
20. CARRASCO L, DE LARA FC, MARTIN DE LAS MULAS J, GOMEZ-VILLAMANDOS JC, PEREZ J, WILKINSON PJ, ET AL. 1996. Apoptosis in lymph nodes in acute African swine fever. J Comp Pathol. 115:415–28.
21. CARRASCO L, BAUTISTA MJ, GOMEZ-VILLAMANDOS JC, MARTIN DE LAS MULAS J, CHACON LF, WILKINSON PJ, ET AL., 1997. Development of microscopic lesions in splenic cords of pigs infected with African swine fever virus. Vet Res., 28:93–9.
22. CARRASCO L, CHACON LF, MARTIN DE LAS MULAS J, GOMEZ-VILLAMANDOS JC, SIERRA MA, VILLEDA CJ, ET AL., 1997. Ultrastructural changes related to the lymph node haemorrhages in acute African swine fever. Res Vet Sci. 62:199–204.
23. SALGUERO FJ, SANCHEZ-CORDON PJ, NUNEZ A, FERNANDEZ DE MARCO M, GOMEZ-VILLAMANDOS JC., 2005. Proinflammatory cytokines induce lymphocyte apoptosis in acute African swine fever infection. J Comp Pathol. 132:289–302
24. Horter, D.C., Yoon, K.J., Zimmerman, J.J., 2003. A review of porcine tonsils in immunity and disease. Animal Health Research Reviews 4, 143–155.
25. IZZATI UZ, INANAGA M, HOA NT, NUEANGPHUET P, MYINT O, TRUONG QL, ET AL., 2021. Pathological investigation and viral antigen distribution of emerging African swine fever in Vietnam. Transbound Emerg Dis. 68:2039–50.
26. SALGUERO FJ, RUIZ-VILLAMOR E, BAUTISTA MJ, SANCHEZ-CORDON PJ, CARRASCO L, GOMEZ-VILLAMANDOS JC., 2002. Changes in macrophages in spleen and lymph nodes during acute African swine fever: expression of cytokines. Vet Immunol Immunopathol. 90:11–22.
27. GOMEZ-VILLAMANDOS JC, CARRASCO L, BAUTISTA MJ, SIERRA MA, QUEZADA M, HERVAS J, ET AL. 2003. African swine fever and classical swine fever: a review of the pathogenesis. Dtsch Tierarztl Wochenschr. 110:165–9
28. FERNANDEZ DE MARCO M, SALGUERO FJ, BAUTISTA MJ, NUNEZ A, SANCHEZ-CORDON PJ, GOMEZ-VILLAMANDOS JC., 2007. An immunehistochemical study of the tonsils in pigs with acute African swine fever virus infection. Res Vet Sci. 83:198–203.
29. JAMBALANG, A. R., OGO, N. I., AGADA, G., OWOLODUN, O., & KUMBISH, P., 2016. Detection of African Swine Fever Virus by Histopathology and Transmission Electron Microscopy. Nigerian Veterinary Journal, 35(4).
30. LINDEN, A.; LICOPPE, A.; VOLPE, R.; PATERNOSTRE, J.; LESENFANT, S.C.; CASSART, D.; GARIGLIANY, M.; TIGNON, M.; VAN DEN BERG, T.; DESMECHT, D.; ET AL., 2019. African swine fever virus hits north-western Europe. Transbound. Emerg. Dis., 66, 54–55.
31. PIKALO J., ZANI L., HÜHR J., BEER M., BLOME S., 2019. Pathogenesis of African swine fever in domestic pigs and European wild boar – Lessons learned from recent animal trials. Virus Research 271:197614, 8 p.
32. NGA BT, TRAN ANH DAO B, NGUYEN THI L, OSAKI M, KAWASHIMA K, SONG D, SALGUERO FJ, LE VP., 2020. Clinical and pathological study of the first outbreak cases of African swine fever in Vietnam, 2019. Frontiers in Veterinary Science. Jul 8; 7:392
33. TIZHE EV, LUKA PD, ADEDEJI AJ, TANKO P, GURUMYEN GY, BUBA DM, TIZHE UD, BITRUS AA, ORAGWA AO, SHAIBU SJ, UNANAM ES., 2021. Laboratory diagnosis of a new outbreak of acute African swine fever in smallholder pig farms in Jos, Nigeria. Veterinary Medicine and Science. May;7(3):705-13.
34. SÁNCHEZ-CORDÓN PJ, FLOYD T, HICKS D, CROOKE HR, MCCLEARY S, MCCARTHY RR, STRONG R, DIXON LK, NEIMANIS A, WIKSTRÖM-LASSA E, GAVIER-WIDÉN D., 2021. Evaluation of lesions and

viral antigen distribution in domestic pigs inoculated intranasally with African swine fever virus Ken05/Tk1 (genotype X). Pathogens. Jun 18;10(6):768.

35. FERNÁNDEZ, A., PEREZ, J., CARRASCO, L., SIERRA, M.A., SANCHEZ-VIZCAINO, M., JOVER, A., 1992. Detection of African swine fever viral antigens in paraffin-embedded tissues by use of immunohistologic methods and polyclonal antibodies. Am. J. Vet. Res. 53, 1462–1467.
36. PÉREZ, J., FERNÁNDEZ, I., SIERRA, M.A., HERRÁEZ, P., FERNÁNDEZ, A., DE LAS MULAS, J.M., 1998. Serological and immunohistochemical study of African swine fever in wild boar in Spain. Vet. Rec. 143, 136–139.
37. SZEREDI L, BAKCSA E, ZÁDORI Z, MÉSZÁROS I, OLASZ F, BÁLINT Á, LOCSMÁNDI G, ERDÉLYI K., 2020. Detection of African swine fever virus in cell culture and wild boar tissues using a commercially available monoclonal antibody. Journal of Virological Methods. Aug 1; 282:113886.
38. GREGG, D.A., MEBUS, C.A., SCHLAFER, D.H., 1995. A comparison of three avidin-biotin complex immunoenzyme systems for detection of African swine fever virus antigen in paraffin-embedded tissues. J. Vet. Diagn. Invest. 7, 17–22.